HYDROLOGICAL PROCESSES AND RUNOFF AT THE ARCTIC TREELINE IN NORTHWESTERN CANADA

P. Marsh, B. Quinton[1] and J. Pomeroy
National Hydrology Research Institute
11 Innovation Blvd.
Saskatoon, Sask. S7N 3H5
[1] also at the University of Saskatchewan, Saskatoon

ABSTRACT

Models of snow accumulation, melt, vertical meltwater percolation, and evaporation, were used in conjunction with observations of basin snow cover and hillslope hydrology to explain certain aspects of the runoff regime, as well as the annual and daily water balance of an Arctic treeline site in northwestern Canada. These studies indicated that snowfall was the largest input to the basin, accounting for 58% of the annual total. However, transport during blowing snow was also significant, accounting for 16% of inputs, while sublimation removed 10% of annual inputs. Although the majority of annual precipitation was released over a brief period in the spring, the initiation of runoff was delayed by the processes of vertical percolation of meltwater into the snow and frozen soil infiltration. As a result of these processes, basin water storage increased dramatically during the early melt period, with over 150 mm of melt occurring before streamflow began. The occurrence of mineral hummocks greatly affected the transfer of meltwater from late lying snow patches, with organic water tracks responsible for rapidly transporting water to the stream channel. Over 90% of annual runoff occurred during the melt period. Surprisingly, however, discharge only removed 44% of snow stored in the basin at the start of melt. The remaining meltwater was stored in the basin, with the majority supplying evaporation, which removed 62% of water inputs to the basin.

INTRODUCTION

Runoff in northern Canada is largely controlled by snow processes. Snowmelt water also carries the fluxes of nutrients and pollutants through northern ecosystems, and supplies freshwater to the Arctic Ocean (Aagaard and Carmack, 1989). The importance of this runoff, and predictions of enhanced greenhouse gas warming in the Arctic (IPCC, 1990), has resulted in an increased interest in modelling these water fluxes . However, Woo (1990) noted that there has been little success in basin scale modelling in permafrost areas. The main problems include: (a) the magnitude of certain processes are different than in more temperate areas, (b) spatial variability is often not well dealt with, and (c) the paucity of data in remote northern areas. Some of the important processes are discussed here.

Tundra snowcover formation is dominated by redistribution of snow by the wind and the resulting snowcover depth is highly variable. During late winter there are typically extensive areas of very thin snowcover, and small areas such as river valleys and hillsides where the snowcover may be several metres thick (Woo et al. 1983; Benson 1982; Pomeroy et al., 1993a). In the Canadian Prairies, Pomeroy et al. (1993b) demonstrated that during blowing snow events, sublimation may remove 30 to 70% of winter snowfall, significantly reducing the amount of snow available for runoff. Redistribution of snow from level areas to gullies or hedges can account for up to 50% of annual snowfall for the prairies. To date, the importance of blowing snow in controlling sublimation and relocation, and therefore snowcover, in northern areas has not been quantified. In addition, the effect of spatially variable snowcovers on melt rates, evaporation, and runoff regime are known to be important. In the high Arctic, for example, Marsh and Woo (1981) demonstrated how numerous large drifts extend the melt period throughout the summer, and result in a glacial type discharge-regime (Church, 1974). The ability to model these effects has not been sufficiently developed.

The re-freezing of meltwater within the snowpack results in a lag between the start of melt and the availability of water for runoff. The magnitude of the re-freezing, and therefore the lag time, is dependent on the snow and soil thermodynamics, with lag time increasing with colder temperatures and higher thermal conductivity of the snow and soil. Although these processes have been documented for the High Arctic, where extreme temperatures increase the lag time by 7 to 10 days, its magnitude in other Arctic regions has not been demonstrated.

During the initial snowmelt period, flow fingers develop at the leading edge of the wetting front (Marsh, 1991) and route water to the base of the pack before the entire pack is wet and isothermal at 0°C. As a result, runoff may occur earlier than if uniform flow occurred, but during this period only a portion of the surface melt is available for runoff. With a spatially variable snowcover, the above processes can result in a significant variation in the timing and magnitude of snowmelt runoff contribution to streamflow. The temporal and spatial variations in these processes have not been described.

Once meltwater reaches the base of the snowpack, it may infiltrate the soil and fill storages, or be available for subsurface or overland flow. Previous work has demonstrated that frozen soil infiltration is highly variable in permafrost environments (Marsh and Woo, 1993) and that surface/subsurface runoff is both temporally and spatially variable (for example: Woo and Steer, 1986 ; Roulet and Woo, 1986; Quinton, 1991; Wright, 1981). A characteristic of vegetated permafrost terrain is the presence of mineral cored hummocks (Mackay, 1980), with the inter-hummock areas dominated by organic material. Since the permeability of the mineral hummocks is several orders of magnitude lower than that of the organic material of the inter-hummock areas and because flow through the later follows tortuous flowpaths, the flow system is very complex. Little is known about the impact of these conditions on the rate at which meltwater is shed from permafrost hillslopes.

The purpose of this paper is to demonstrate the role of snow accumulation and melt, and slope runoff in controlling the magnitude, rate, and timing of snowmelt runoff from a typical basin in the low Arctic tundra zone in northwestern Canada. Each of these processes will be described, and their impact on runoff, evaporation, and basin water balance demonstrated.

STUDY SITES

During the spring and summer of 1993, measurements were carried out in a biophysically representative sub-basin (Siksik Creek) of the Trail Valley Creek (TVC) research basin (Figure 1), located approximately 40 km north-northeast of Inuvik. The climate is characterized by short cool summers, long cold winters, and low precipitation, much of which occurs as snow (Table 1). Heginbottom and Radburn (1992) mapped the permafrost in the study area as continuous, with talik zones only occurring beneath lakes. Permafrost depths are up to 350 m , and active

Figure 1. The Trail Valley Creek gauging station is shown by (⇨). Also shown is the TVC basin boundary, and the location and flow direction of Siksik Creek (←).

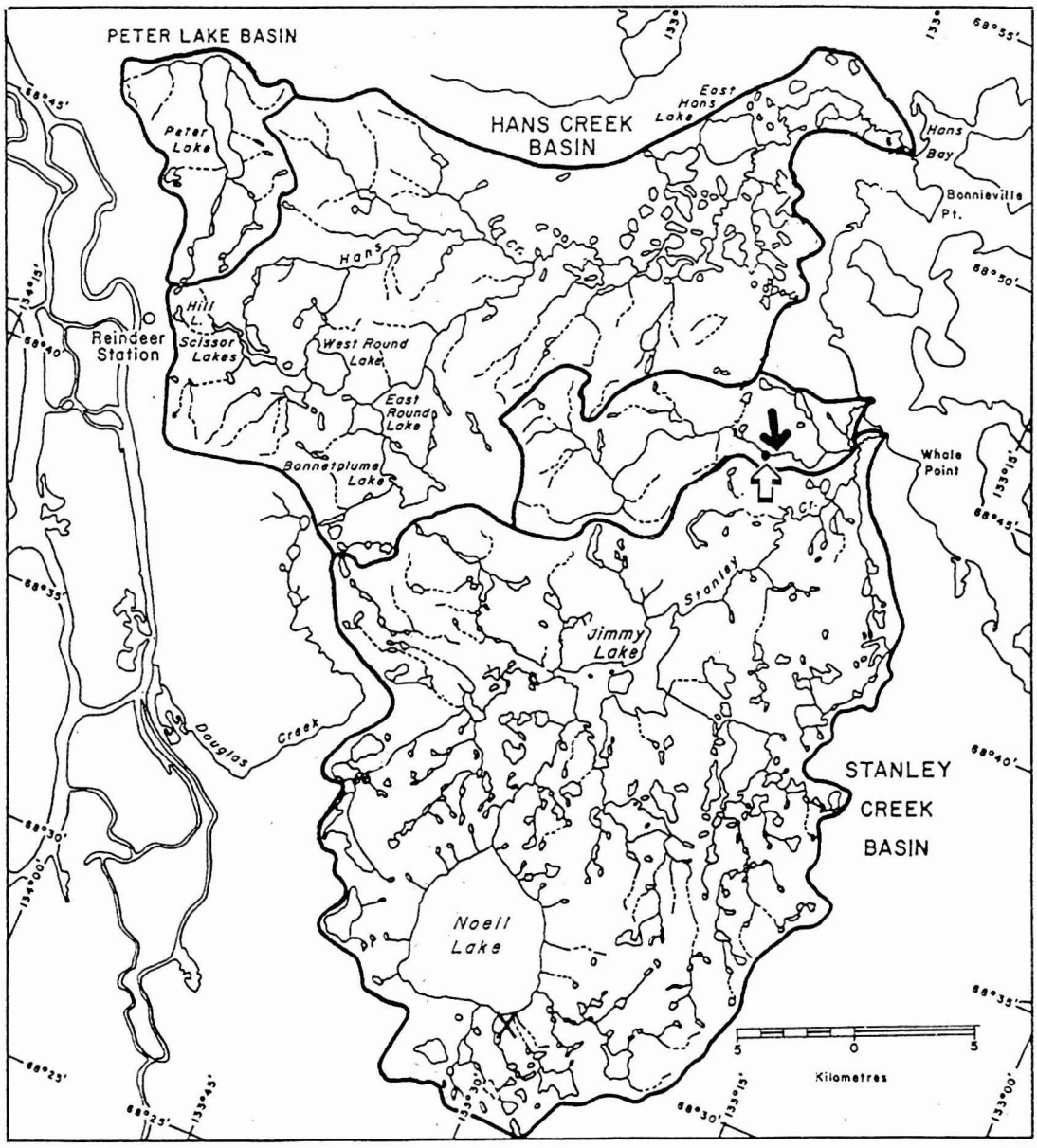

layer depths vary from 0.3 to 1.0 m. The ground surface is dominated by numerous periglacial features such as ice-wedges, earth hummocks, and thermokarst phenomena for example.

Trail Valley Creek is approximately 63 km^2 in area with elevations ranging from 60 to 190 m asl. The stream channel occupies an abandoned meltwater channel carved into a plateau (Rampton, 1974). The Siksik Creek sub-catchment is located in the lower section of TVC, has

Table 1 - Climatic conditions in the study region (Atmospheric Environment Service 1982a, 1982b). Tuktoyaktuk is located on the Beaufort Sea coast (approximately 80 km north of Trail Valley Creek), while Inuvik is approximately 40 km south of Trail Valley Creek..

Location	Mean Daily Temperature (°C)			Precipitation (mm)			Rain (mm)	Snow as a % of total precip
	Annual	(D,J,F)	(J,J,A)	Annual	Oct. to Ap.	May to Sept.		
Inuvik	-9.8	-28.6	11.5	266.1	123.9	142.2	114.6	56.9
Tuktoyaktuk	-10.9	-27.6	8.2	137.6	56.2	81.4	72.3	47.5

lower relief than TVC, but has more short, steep slopes, and is 0.83 km^2 in area (above the middle weir).

Variations in the relative contributions from the major hillslope runoff pathways (eg. overland flow, matrix seepage, macropore flow) were studied at a biophysically representative hillslope plot. The study plot is east facing, and during the snow accumulation period a deep drift (water equivalent > 1000 mm) develops on the upper slope. The middle and lower portions of the slope have much shallower snowpacks (water equivalents < 200 mm); and these areas become snow free roughly one month before the upper slope.

The surface of the plot is covered with mineral earth hummocks. In the upper portions of the slope, the hummocks are roughly 1 m in diameter, with crest heights between 20 and 40 cm above the surrounding hollows. The hummocks are bare or support a thin lichen layer. Lower on the slope, the frequency of hummocks increases, but their average diameter and height decrease. In addition, the number of sedge tussocks (Eriophorum spp) increases.

Throughout the slope, the interhummock zones are comprised of organic soils (peat depths generally less than 40 cm) supporting bryophyte, graminoid, and herbaceous species. The hydraulic conductivity (K) in the interhummock zones ranges between 10^{-3} to 10^{-6} m s^{-1}, with

lower values occurring at depth where humification and decomposition are more advanced; while for the mineral hummocks, K is $< 10^{-7}$ m s^{-1}.

Because of ~~Due to~~ the low hydraulic conductivity of the mineral matrix, flow is limited to the following subsurface pathways within the organic interhummock zones: matrix non-water track flow (MNWT); matrix water track flow (MWT); and, macropore water track flow (MPWT). Water tracks are defined as the interhummock zones, while non-water track flow occurs where hummocks are sufficiently sparse so that their effect on subsurface flow through the interhummock zone is negligible.

METHODS

Field Observations

Premelt Snow Distribution

Snow depth and densities were sampled from representative landscape types in Trail Valley Creek and Siksik Creek during April and May, 1993, just prior to melt. These stratified surveys followed the technique described by Steppuhn and Dyck (1974) and Woo et al. (1983), using landscape types defined for the region by Pomeroy et al. (1993a). Twenty-five depth measurements and five density measurements were taken at 5-m intervals in each of the following landscape types: a) tundra, b) high shrub, c) open forest, d) closed forest, e) sheltered valleys and f) drifts. Whilst all landscape types are found in Trail Valley, only tundra, high shrubs and drifts are found in Siksik Creek.

Landscape classes were derived and mapped for Trail Valley Creek and Siksik Creek using a digital terrain model, aerial photographs of late spring snowdrifts, a mid-summer Landsat Thematic Mapper image and *PCI* software for image classification. The red and four infrared bands from Landsat were used for the vegetation classification. Areas of water, open tundra, high shrubs, taiga, forest, wetland and bare soil were identified from the satellite image. Drift areas in Trail Valley Creek were identified as slopes of gradients greater than 9% in areas having an open upwind fetch. For greater spatial resolution in the smaller Siksik Creek, the remaining drifts identified from aerial photographs taken in mid-June, 1992 were registered onto the

landscape classification. The landscape classification was compared to aerial photographs and ground observations and found adequate for the purposes of hydrological modelling. The percent cover for each basin is given in Table 2, and the resulting landscape classification map for Siksik Creek is shown in Figure 2.

Snow Distribution during Melt

A series of aerial photographs of Trail Valley and Siksik Creeks were taken on clear days during the melt, 22, 25, 30 May and 3 June (JD 143, 145, 150, 154). These photographs were aggregated (four per aggregate image), digitally scanned and analyzed using *Mocha Image Analysis* software. The proportion of the landscape covered by snow, perimeter to area ratio of the remaining snowpatches and fractal dimension (an index of irregularity) of the snowpatches were calculated for each aggregate using techniques described by Shook et al. (1993).

Meteorological measurements

Data from a meteorological station installed in the Siksik Creek basin, was used for estimating snow accumulation, melt and summer evaporation. This station is on a tundra plateau in the middle portion of the basin. The parameters measured and recorded half-hourly are: air temperature, relative humidity, wind speed at four levels up to a 3-m height, wind direction, net radiation, incoming and outgoing solar radiation, snow depth (Campbell Scientific acoustic snow depth gauge), air pressure, blowing snow particles (Brown and Pomeroy, 1989), and snow/soil temperature at 5 levels down to a depth of 0.75 m. Snow depth at this site was approximately 0.4 m, and as a result, became snow-free relatively early in the melt period (May 28, JD 148). To supplement this record, a portable meteorological station was installed over a deeper snow patch (0.6 m) which retained its snowcover until approximately June 7 (JD 158).

Unfortunately, continuous records of net radiation are not available from the permanent meteorological station. During most of the period, net radiation was available from the portable station. However, for certain periods during the summer, net radiation was estimated using a relationship between net solar radiation and net radiation.

Figure 2. Siksik Creek basin landscape map as derived from Landsat image and digital elevation model.

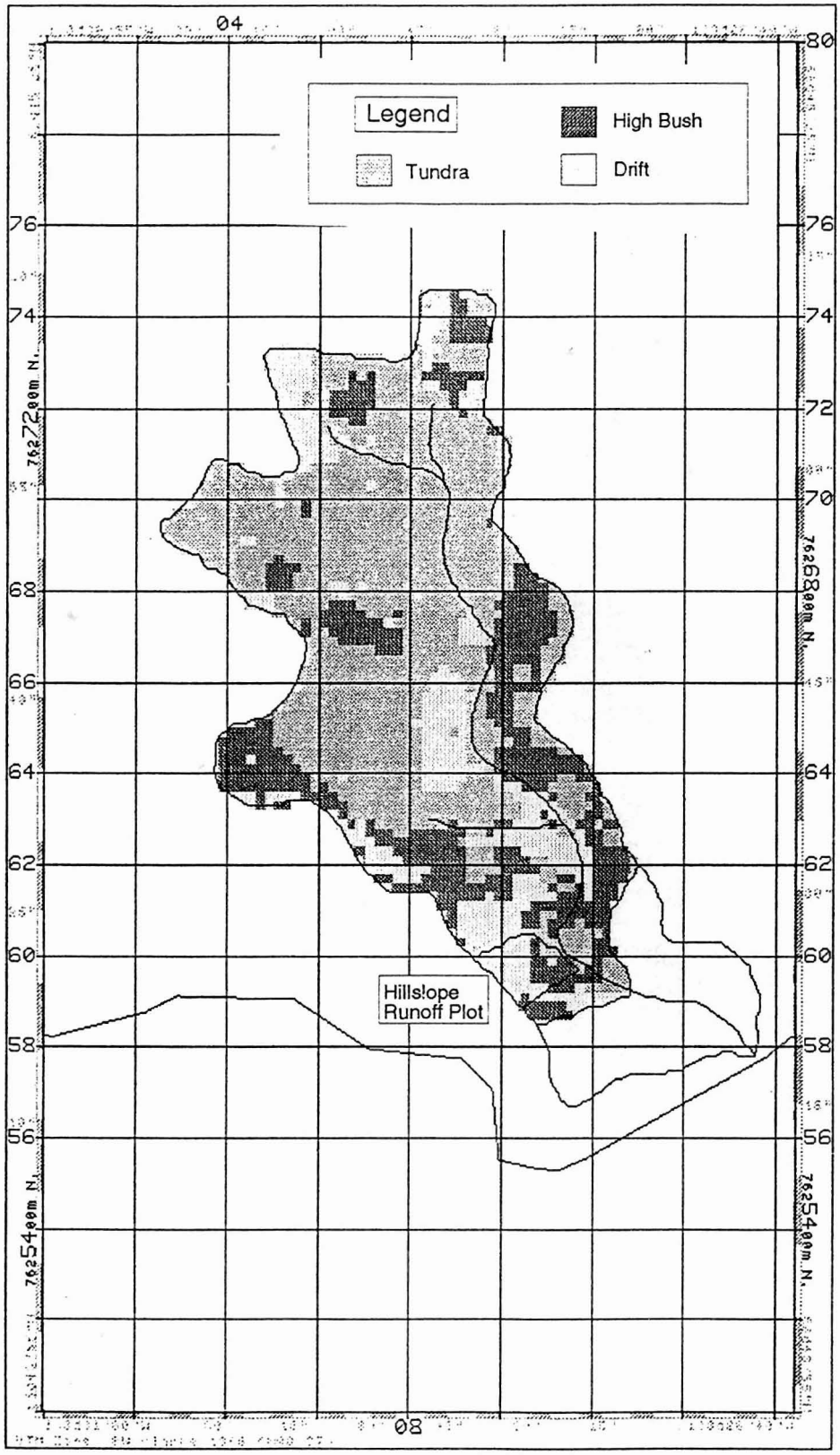

Vegetation Cover and Topography

Table 2 - Landcover types for Trail Valley and Siksik Creek basins

Basin	Tundra	High Bush	Forest	Drifts
Trail Valley	75%	16%	0.7%	8%
Siksik	59%	24%	0%	17%

Stream discharge

Siksik Creek was gauged at three 90° v-notch weirs, separating the basin into three segments. This paper will only report on data from the middle weir. Since the stream channel is filled with 1-2 m of snow at the start of melt, the weir was dug free of snow prior to the start of discharge. Observations showed that stream discharge began as saturated flow through the snow clogged channel long before surface flow occurred. If the v-notch weir had not been excavated, this initial period of discharge would not have been observed, and the annual discharge underestimated. Discharge measurements were conducted using standard velocity-area methods using calibrated Price current meters. Water level is recorded using a Type-F float- chart recorder. Early in the runoff period, only discrete discharge measurements were made because of wide spread channel flooding.

Hillslope runoff

A continuous record of surface runoff was obtained at the study plot through the use of overland flow collectors which diverted surface flow toward a flume box equipped with a Stevens Type-F stage recorder. Macropore discharge estimates were routinely made at the outlets of 10 macropores along Siksik Creek streambank using a variety of methods. Continuous measurements were made using a tipping bucket mechanism connected to a Campbell 21X datalogger. Where this method could not be employed (due to high flow rates or technical difficulties introduced by the macropore outlet location) timed volumetric flow measurements were made. Subsurface matrix flow velocities through the interhummock zone were estimated from chloride tracing experiments. Roughly 80 litres of 500 ppm KCl was applied to the surface along a 20 metre transect running perpendicular to the hillslope, 10 m upslope from the

streambank. In situ chloride concentrations were monitored downslope using chloride sensing micro-probes manufactured at NHRI (Farrell et al., 1991). Six micro-probes were inserted to the base of the active layer near the streambank, downslope of the transect. Two representative sites for each of the three major subsurface flowpath types were used. A macropore with a relatively high flow rate (macropore 9), and one with a medium flow rate (macropore 6) were chosen to represent macropore water track subsurface flow. The probes were inserted into the surface sediment layer at the macropore outlets. The micro-probes were wired to a Campbell 21X datalogger for continuous recording. The chloride tracing experiment was repeated five times between June 2 and July 30. For each experiment, the subsurface flow velocity at each probe location was calculated by dividing the straight-line distance from the application transect by the time required for the chloride breakthrough curve peak to pass by the sampling location.

In the lower, middle and upper slope, ablation and surface snow density measurements were made in order to calculate daily snow water equivalent storage loss and melt contributions to the plot. The water table in the lower plot was measured daily at first, and then continuously once a Stevens Type-F recorder was installed. Active layer depth was measured twice weekly along a transect which ran from the streambank to the upper slope.

Modelling

Snow accumulation, relocation, and sublimation

Blowing snow was modelled using a simplified version of the Arctic Blowing Snow Model (Pomeroy et al., 1994). The ABSM conducts a mass balance of blowing snow using a control volume over specific landscape types. Inputs to the control volume are incoming blowing snow transport, snowfall and surface snow erosion, outputs are blowing snow transport, sublimation and surface snow deposition. Two types of Arctic terrain are specified, sources and sinks. Source areas, such as tundra, experience erosion or deposition of snow and can have transport and sublimation out of their control volume, whilst sinks (drifts or high shrubs) experience only deposition and have no flux out of their volume. Monthly fluxes of blowing snow transport and sublimation for source area are modelled using a regression algorithm that simulates the monthly output of a physically-based blowing snow mass balance model (Pomeroy

and Gray, 1994; Pomeroy et al., 1993b). The model uses the monthly means of wind speed, daily maximum temperature, daily minimum temperature, daily maximum relative humidity, daily minimum relative humidity, depth of snowcover and the monthly snowfall. These data were derived from the meteorological station at Trail Valley Creek, except for monthly snowfall which was reconstructed in the following manner. Monthly snowfall records from the Inuvik AES Climatological Station (40 km south) were obtained and totals compared to sheltered areas in Trail Valley Creek which were affected by neither blowing nor intercepted snow. The Inuvik October through May snowfall was 131 mm SWE whilst 190 mm SWE accumulated in Trail Valley. Presuming underestimation of snowfall at Inuvik (Goodison, 1978), the monthly snowfall record was reconstructed using the annual ratio of "true" snow accumulation to Inuvik AES snowfall to correct the monthly snowfall values from Inuvik.

The ABSM was applied to tundra, high-shrub, taiga, forest and drift landscapes in Trail Valley Creek and Siksik Creek. Snow fluxes for the tundra used a mean fetch length of 1.45 km (derived from topographic data and the vegetation classification) and the results of the transport and sublimation algorithms. Monthly snow accumulation is monthly precipitation less monthly transport and sublimation losses. The high-shrub and taiga landscapes were presumed to lose no snow to wind transport but to receive 10% of that transported from the tundra. The mean fetch of high-shrub or taiga is set at 100 m (derived from the vegetation classification) and incoming blowing snow is distributed evenly over this fetch and added to monthly precipitation to calculated monthly accumulation. Drift areas lose no snow to transport and as transport is bi-directional and perpendicular to Trail Valley, each drift receives 40% of the snow transport off a 1.45 km upwind fetch of tundra. This incoming blowing snow is evenly distributed over the 50-m length of drift (length derived from ground surveys) and is added to monthly precipitation to calculate monthly accumulation.

Snowmelt and Vertical Percolation of Melt Water

The surface energy balance during melt was determined using meteorological data collected from the two masts described earlier. The radiation fluxes from these masts were distributed using the basin snowcovered area as determined from aerial photographs. Net radiation was measured over the snowpatch whilst incoming and outgoing shortwave radiation

were measured over the bare ground. Measurements over the snowpatch represented a 100% snowcovered net radiation flux, hence the component shortwave flux was adjusted to reflect actual basin snowcover. The snowpatch was assigned an albedo (α_s) of 0.7 (average from measurements) and non-snowcovered areas assigned an albedo (α_g) of 0.2 (average from measurements). The net shortwave flux over the snowpatch was found as ($1-\alpha_s$) x incoming shortwave, the net longwave flux over the snowpatch is therefore the residual. Net radiation over the basin is therefore the longwave flux (errors in estimating this from the snowpatch longwave flux are relatively small) plus the incoming shortwave less the average (weighted by snowcovered area) outgoing shortwave flux. This procedure is abandoned when snowdepth at the snowpatch is less than 5 cm, at this point the unaltered net radiation from the snowpatch is used to drive snowmelt. Surface energy balance was then estimated from bulk aerodynamic methods as outlined by Dunne et al. (1976), Moore (1983), and Heron and Woo (1978). The daily melt contribution to runoff was calculated by weighting the calculated daily melt by the snowcovered area.

A model of vertical percolation of melt water into snow as described by Marsh and Woo (1984b) was used to calculate the availability of water for runoff at the base of the snowpack. This model parameterizes the processes of water flux through cold, dry snow as follows. The wetting front is idealized as a two component wetting front. The background front, above which all snow is wet and isothermal at 0°C, and a finger front representing the deepest penetration of flow fingers. Field studies have demonstrated that flow fingers vary in size only over a very small range of sizes, and that on average, they cover 22% of a horizontal surface, while carrying 48% of the total flow (Marsh and Woo, 1984a). During infiltration, ice layers are allowed to grow at pre-melt strata boundaries. With the rate of growth controlled by the temperature gradient above and below the strata boundaries. This temperature gradient is determined from modelling the snow and soil temperature, and soil heat fluxes. Data used in this model include surface melt, snow and soil temperature at the start of melt, and snow and soil thermal properties calculated using the methods described by Marsh and Woo (1984b).

Evaporation

Evapotranspiration for the snow free period was estimated using the Priestley-Taylor

equation (Priestley and Taylor, 1972; Rouse et al., 1987). Air temperature and net radiation were measured at the meteorological stations. Ground heat flux was estimated from changes in measured soil temperature plus the latent heat used for deepening the active layer (Rouse, 1984). The α parameter relating equilibrium evaporation to actual evaporation was estimated from nine small lysimeters (47.8 cm^2 in area) located in representative vegetation and covering a range of surface wetnesses. During the snowmelt period, evaporation from the snowfree areas was estimated by weighting evaporation by the measured proportion of the basin snowfree area.

HYDROLOGIC PROCESSES

Snow cover accumulation, relocation, and sublimation

Differing landscape configurations caused the snow accumulation fluxes in Siksik Creek to differ from Trail Valley Creek. Trail Valley Creek is dominated by tundra plateaus (75%) and has only 7.8% of its area occupied by snow drifts. Siksik Creek is more dissected and hence has less tundra (59% of its area) and more drifts (17%). As shown in Figure 3, tundra snow underwent a severe transformation by blowing snow. Only 55% of cumulative snowfall

Figure 3. Bar plot showing the SWE for precipitation, sublimation, transport, and accumulation for each landscape type in Siksik Basin, and for the entire basin.

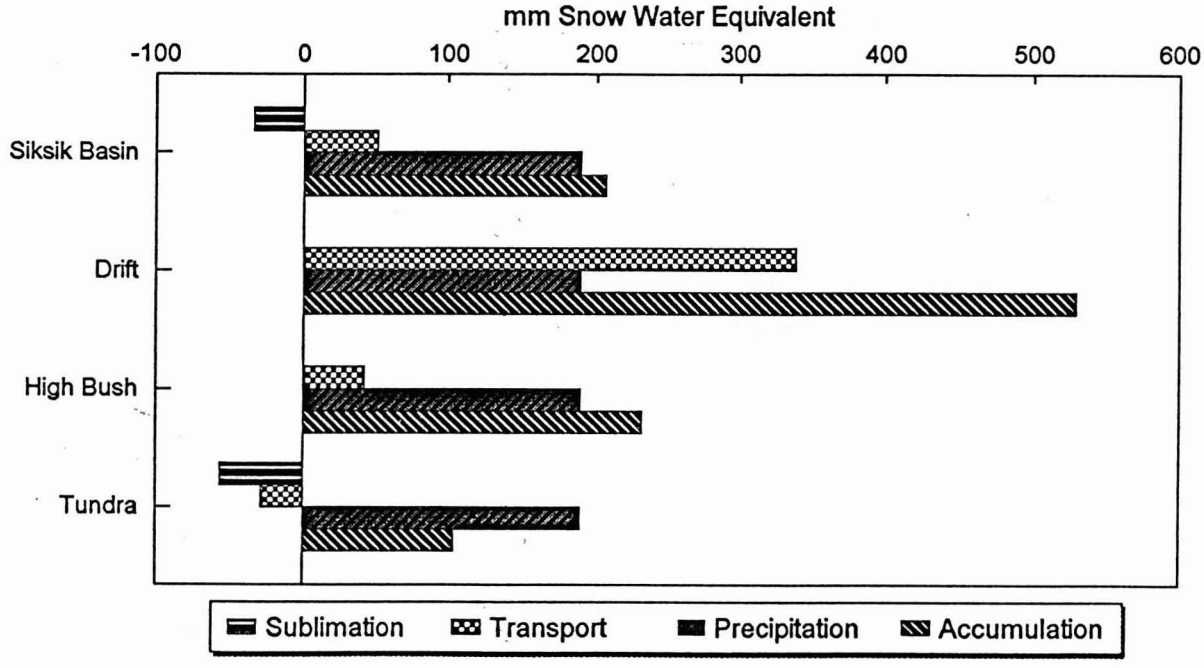

remained as snowcover in this landscape type. Of that removed, 57 mm SWE (two-thirds) sublimated and 29 mm SWE (one-third) was transported to drifts or high shrubs. The high shrub area received an additional 42 mm SWE of snow from transport, equivalent to over one-fifth of snowfall. Modelled accumulation in the high shrub was 8% less than that measured in the snow survey. Compared to landscape-stratified snow surveys the Arctic Blowing Snow Model overestimated tundra snow accumulation by 34%, possibly due to an undermeasurement of wind speed when anemometers became ice-covered in mid-winter. Drift snow was also strongly transformed by blowing snow. The blowing snow transport input to drifts was 339 mm SWE, over 1.5 times greater than the precipitation input. The ABSM underestimated drift snow accumulation by 17%, again possibly due to undermeasurement of wind speed. Whilst the errors in ABSM estimates of snow accumulation in each landscape type are not small, they do compensate for one another, hence the difference between the weighted basin-wide snow water accumulation derived from snow surveys and that derived from the ABSM output is 1.5 mm SWE, less than 1%. Because tundra is less dominant in Siksik Creek than in Trail Valley Creek, the level of agreement is much better in Siksik than in Trail Valley, where the difference in accumulation between model and measurements is 12% (Pomeroy et al., 1994).

Snowmelt and vertical percolation of meltwater

Snow melt began when air temperature rose above 0°C in May (Figure 4), with the first day with significant melt occurring on May 15, 1993 (Julian Day 135). Low rates of melt occurred over the next 5 days, but then melt ceased for 4 day period when air temperatures were below 0°C between May 20 and 24 (J.D. 140 to 143), and resuming on May 24 (JD 144). During this period, melt rates gradually increased, reaching a maximum value of over 60 mm/day, and snow cover gradually decreased from 98% on May 17 (JD 137) to 88% on May 22 (JD 142) (Figure 4). As melt rates increased, snow covered area decreased to 12% over the next 8 days. After this time, snowcover gradually decreased, and all snowpatches were melted by approximately early July.

The snow percolation model was used to estimate the initiation of the timing of runoff for each landscape class within Trail Valley and Siksik Creeks. The mean snowcover depths varied from 45 cm for tundra, 100 cm in high bush areas, to 185 cm for drifts. Likewise, densities were

Figure 4. Air temp, net radiation, measured basin snow cover, and calculated snowmelt. The date of the start of streamflow (S), the peak flow (P), and when diurnal snowmelt cycles were no longer visible (ND) in the discharge record are shown for Siksik Creek. The lower three diagrams shown the predicted movement of the finger wetting front (FF) and the background wetting front (BF). The arrival of these fronts at the snowpack base indicate the dates when each snowcover was not contributing water (NC), when it was partially contributing (PC), and fully contributing (FC) meltwater to runoff.

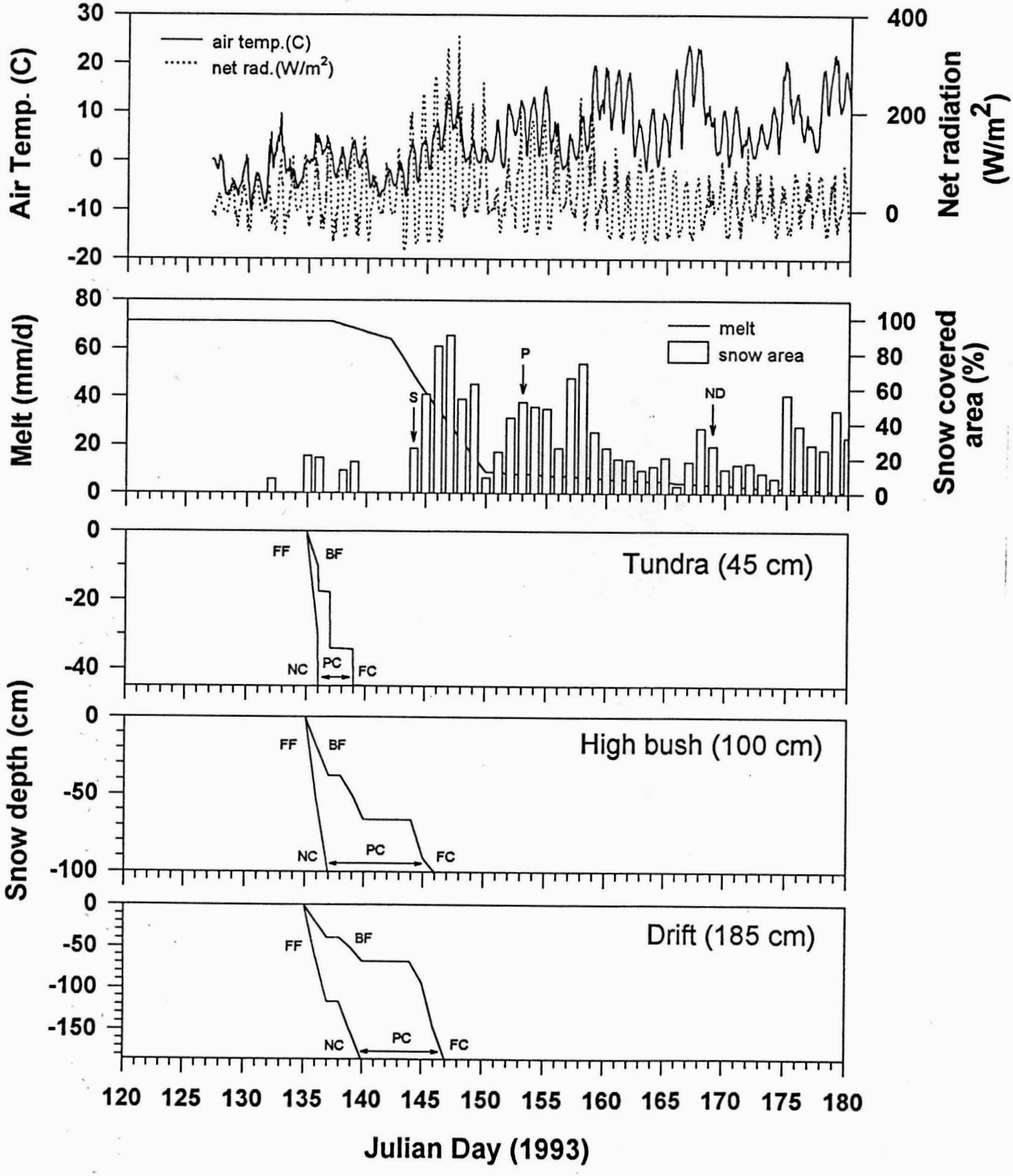

150, 190, 230 and 250 km/m^3 respectively. Figure 4 illustrates the background (BF) and finger wetting front (FF) advances, and the availability of meltwater at the base of the snowpack for each landscape class. Meltwater first reached the base of the snowpack, and therefore was available to infiltrate the frozen soil or to runoff, at tundra sites on May 16 (JD 136), only one and a half days after the start of melt. The background front however, did not reach the base of the pack until May 19 (JD 139). The drift areas were at the other extreme, with the finger front not reaching the base of the snowpack until May 20 (JD 140), 5 days after the start of melt. At these sites, the background front reached the base of the snowpack 7 days later. The high bush was intermediate between these extremes (Figure 4).

During the period after the finger front reaches the base of the pack, but before the background front does, only a portion of the surface melt is available for infiltration or overland flow (Marsh and Pomeroy, 1994). Field measurements suggest that during this period only half the surface melt is reaching the snow base. The tundra site was partially contributing for about 3 days, while the drift for only 7 days. Only once the background front reaches the base is all surface melt available.

Hillslope runoff

Once water is available at the base of the snowpacks, it may infiltrate the soils and/or be available for overland flow. Although there are no direct measurements of frozen soil infiltration, indirect evidence suggests that all meltwater from the tundra snowpacks infiltrated the frozen soils during the few days after water was available at the snowpack base (starting May 16; JD 136) (Figure 4). During this period, no surface water occurred at the hillslope, implying that it all infiltrated the frozen soils. This gives a lower limit for frozen soil infiltration of approximately 100 mm (ie. equal to the tundra snowpack water equivalent).

Although runoff from the slope began as subsurface flow through the organic pathways while the slope was still snow covered (Marsh and Quinton, 1993), significant flow did not begin until after the removal of the tundra snowcover on the lower portion of the slope (approximately May 22 or JD 142). After that time, the active layer began to deepen rapidly, and meltwater was contributed from the drift (Figure 4) on the upper portion of the

slope. This resulted in the water table remaining near the ground surface, the occurrence of sub-surface flow, and the initiation of overland flow by May 25 (JD 145) (Figure 5). During the next 4 days, overland flow gradually increased, with a peak flow occurring on May 27 (JD 147), coinciding with a high melt day and after the drift was full contributing (Figure 4). Over the next 3 days, melt was low (Figure 4) and overland flow likewise decreased. After May 31 (JD 152), snowmelt again increased in response to rising temperatures (Figure 4), resulting in a similar response in overland flow (Figure 5).

Figure 5. Surface discharge from the study plot (a); and Siksik Creek discharge (b) during the spring melt period. For the remainder of the summer, Siksik discharge was very low, with only a few small increases due to rain.

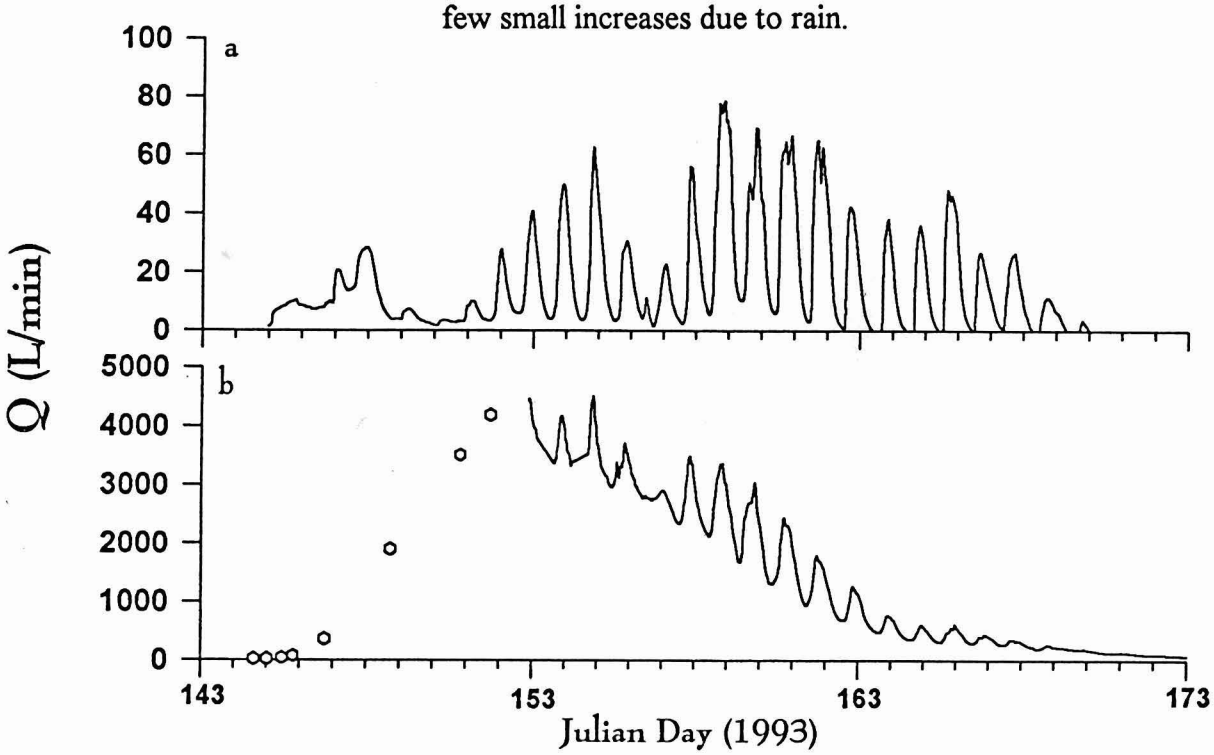

Runoff from the slope during this period was also affected by the relative importance of the various flowpaths. The low hydraulic conductivity (K) of the mineral hummocks promotes preferential flow through the interhummock zone. Hence, the residence time of water following subsurface flowpaths depends largely on the conducting efficiency of the interhummock zone, which in turn is governed by the size, density and spatial distribution of the mineral hummocks. As hummock density increases, the interhummock zone becomes increasingly fragmented. This results in local variations in flow velocity as runoff follows

increasingly tortuous pathways around the mineral hummocks, which are essentially obstructions to flow.

The impact of hummocks on the two types of water track flow (MWT and MPWT) depends upon their size, density and spatial distribution. Macropore water track flow occurs mostly in the near stream zone where many water tracks contain natural horizontal pipes. These macropores (diameters of 5 to 20 cm) become viable flowpaths once intersected by a rising water table. When macropores are non-conducting, both water track types conduct flow at a rate limited by the matrix hydraulic conductivity. However, since the flow rate through macropore water tracks is equal to the sum of matrix seepage and macropore flow, once macropores begin to conduct, the rate of increase in flow per unit rise in hydraulic head is much larger in water tracks that contain macropores than in those that do not. Figure 6 illustrates the simultaneous flow rates of matrix seepage as illustrated by a chloride breakthrough curve, and macropore flow of a macropore water track at the streambank.

6. Simultaneous flow through the matrix and macropore of the water track containing macropore 6. Matrix flow is illustrated by the chloride breakthrough curve as sensed by a micro-probe inserted into the watertrack matrix, and macropore flow is measured by a tipping bucket mechanism positioned at the macropore outlet.

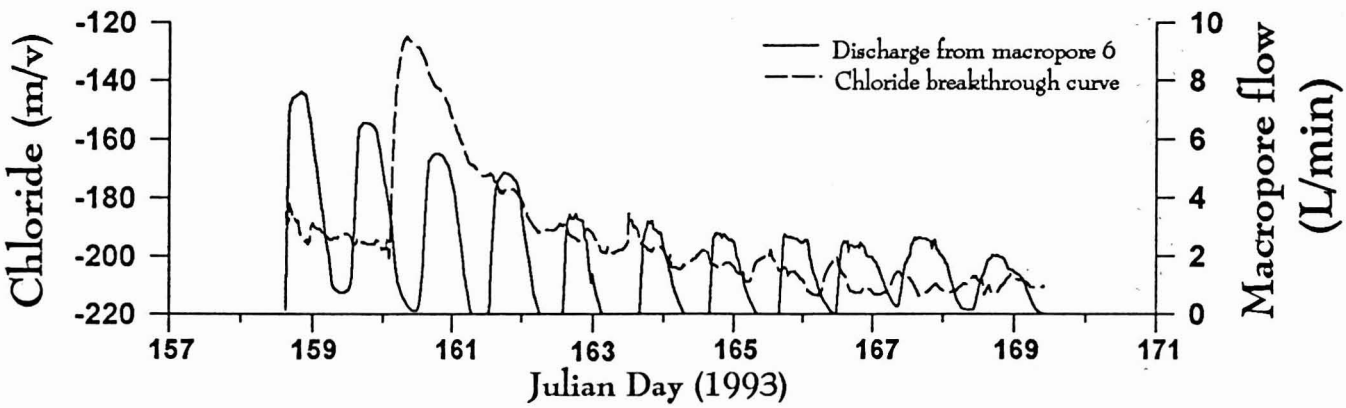

Figure 7 shows the flow velocities calculated for six chloride probe locations within the interhummock zone (two of each for MNWT, MWT and MPWT flowpaths) for the five dates when chloride tracing experiments were conducted. In all cases, either the MPWT (four cases) or MWT (one case) have the highest flow velocities. MNWT conducts at the lowest rate in all

7. Subsurface flow velocities for the three major subsurface flowpath types calculated from repeated chloride tracing experiments. For the MPWT flowpaths, the left bar is for macropore #9 and the right for macropore #6.

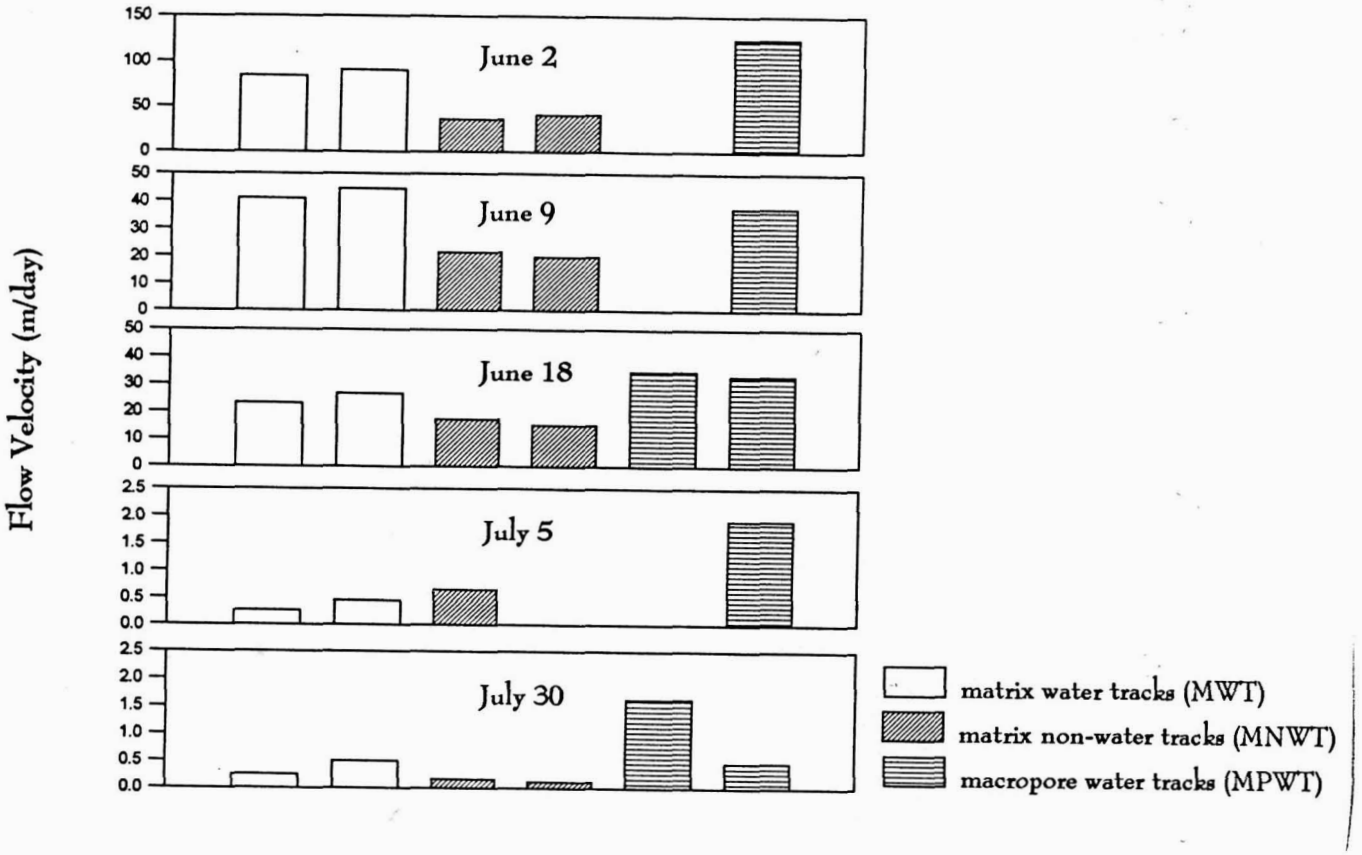

but one case. These data show that: i) the three major subsurface flowpaths conduct at different velocities; ii) the relative velocities through these flowpaths change with time; and iii) the flow velocity of individual flowpaths changes with time (Figure 7). Understanding these changes requires a consideration of the changes in snowmelt rate, active layer development, and water table elevation (Figure 8).

The middle and lower slope of the study plot (where the chloride probes are located) were snow free for all five tracing experiments. However, the deep snow drift in the upper portion of the hillslope persisted in contributing runoff water for the first three tracing experiments. Figure 7 shows that these periods demonstrate the least variation in the relative flow rates of the three flowpath types. The importance of the late-lying snow drift on hillslope runoff is emphasized by the fact that within one day of it's disappearance, the groundwater table falls off dramatically, and flow from macropore 6, as well as overland flow cease (Figure 8).

Figure 8. Snow water equivalent storage and melt from the lower, middle and upper slope (a); water table depth (b); and active layer development for mineral (hummocks) and organic (interhummock zone) soils (c).

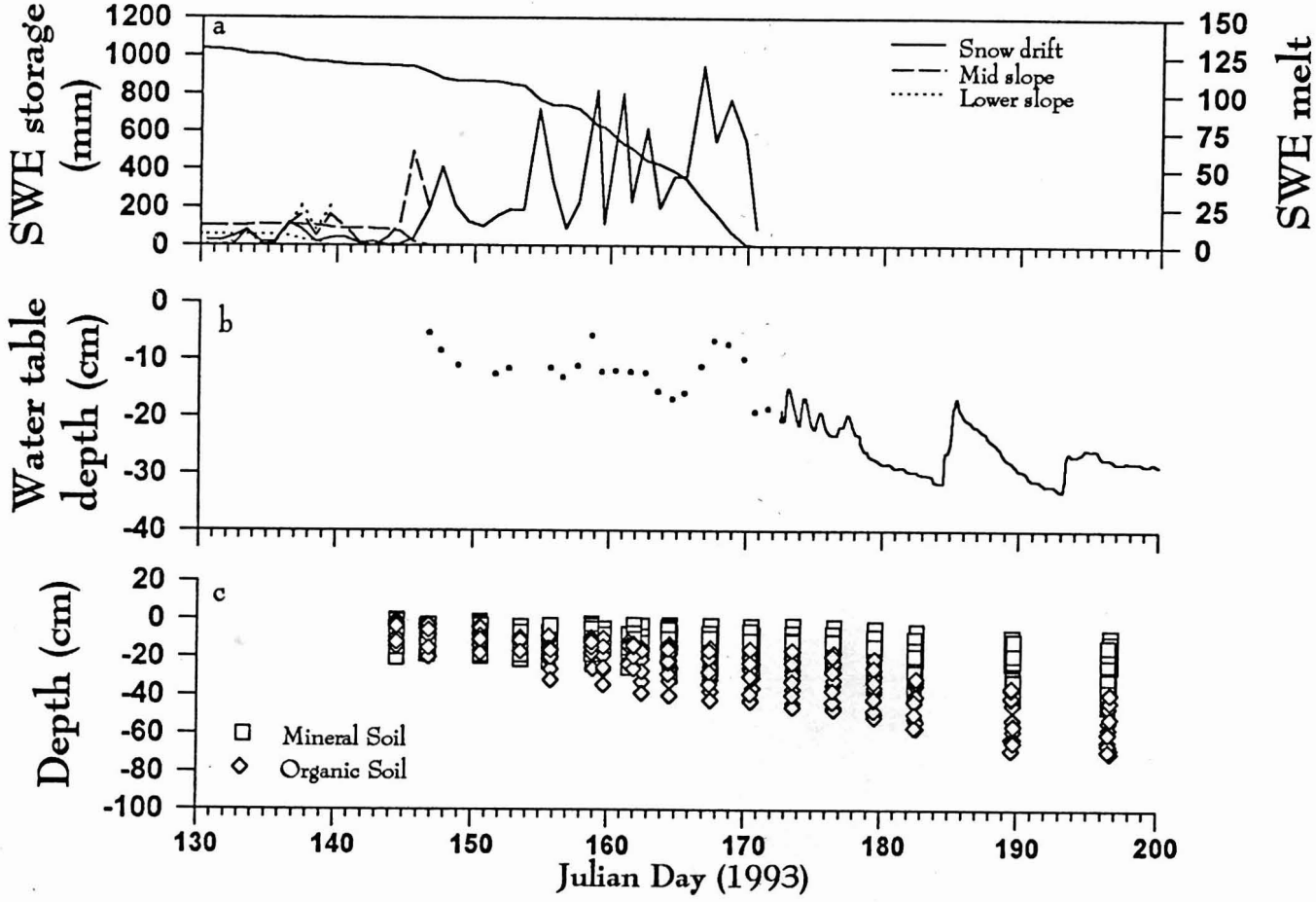

For the first three experiments, the presence of the melting snow drift kept the water table high enough (8 to 12 cm below surface) to intersect the zone of living vegetation (10 to 15 cm thickness). This enabled MWT flow to occur at a rate comparable with overland flow. Thus MWT and MPWT flow rates during this period were similarly high (Figure 7).

Experiments 4 and 5 were conducted following the complete ablation of the late-lying snow drift. With the cessation of snowmelt input to the top of the study plot (groundwater levels which were roughly 10 cm below the surface during the first three experiments) fell to 20 cm and 32 cm below the surface for Experiments 4 and 5 respectively. Over the same period the average active layer depth in the interhummock (organic) zone increased from 30 cm during Experiment 3, to approximately 60 cm by Experiment 5 (Figure 8).

The cessation of melt input in combination with a deepening active layer resulted in a

rapidly falling water table after June 18 (JD 169). Because K decreases exponentially with depth in peat soils (Chason and Seigel, 1986), a falling water table not only results in lower hydraulic head gradients, but also a marked decrease in the average K of the saturated zone. Consequently, as the elevation of the water table decreases, horizontal flow rates fall dramatically. For example, the flow rates during Experiments 4 and 5 are 2 to 3 orders of magnitude lower than during experiment 1, and 1 to 2 orders of magnitude lower than experiments 2 and 3.

On July 5 (JD 186), Macropore 6 was still conducting, and thus it's flow rate remained relatively high (Figure 9). However, by July 30, flow through Macropore 6 had ceased, and the MPWT flow rate reduced to a level comparable to the MWT flowpaths. Macropore 9 was still conductive on July 30, hence the higher flow rate of that MPWT flowpath.

Figure 9. Discharge from macropores 6 (continuous) and 9 (discrete).

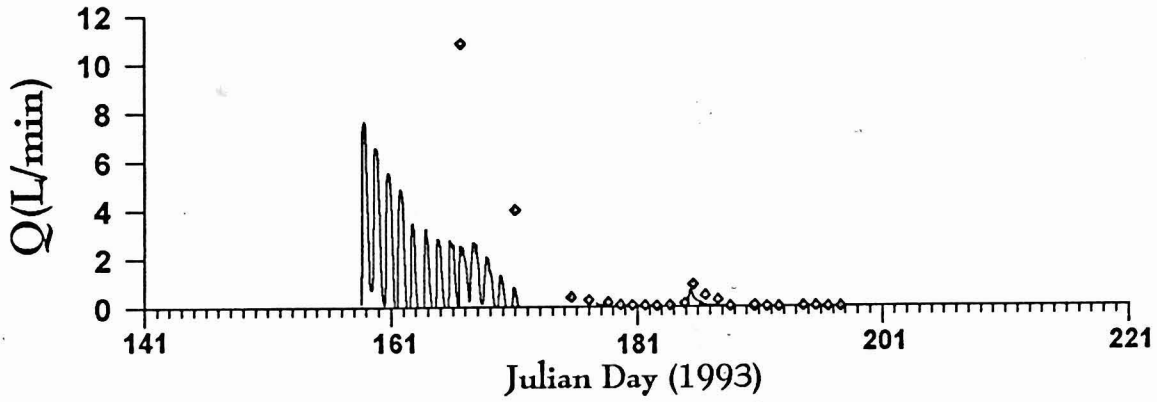

Overland flow discharges from the plot in diurnal pulses that are synchronous with macropore 6, but the flow rates are an order of magnitude larger. The overland flow and macropore 6 peaks also occur on the same date, but the former ceases one day prior to the cessation of flow from macropore 6. Macropore flow is prolonged since the elevation of the macropore outlet is lower, and therefore the declining water table falls below the elevation of the drainage channel first.

The diurnal pulses of overland flow are synchronous with those of Siksik Creek (Figure 5), but far more pronounced. For overland flow the diurnal lows approach zero, and for the final week, flow starts and stops diurnally. Overland flow is effected far more severely by the two periods with reduced melt rate (May 28-30 [JD 149-151] and June 4-5 [JD 156-157]), because of

the larger channel storage of Siksik Creek which dampens the relative magnitude of diurnal fluctuations.

Overland flow stopped on June 19 (JD 170), but the Siksik Creek recession limb continued until July 4 (JD 185), when flow which was negligibly small rose in response to rainfall. During this period, Siksik continued to receive subsurface contributions, and diurnal fluctuations streamflow ceased by June 18 (JD 169).

Siksik Creek peakflow occurred on June 2 (JD 153), while the overland flow peak occurred nearly 1 week later on June 8 (JD 159). This difference is probably due to the existence of the large drift which occupies >50% of the slope plot (Figure 2). In comparison, drifts covered only about 17% of Siksik basin. It is likely that the early overland flow, and the rise to the peak flow of Siksik Creek were driven by snowmelt from the tundra areas with shallow snowcovers which had completely melted by approximately May 24 (JD 144). As shown earlier, these areas began to contribute water to snowmelt soon after the start of melt. However, the drift was not completely contributing until May 27 (JD 147), after the tundra snow had disappeared (Figure 4).

(5) Hydrologic regime

Water balance

The annual basin water balance of Siksik Creek is given by

$$(1) \qquad (P_S \pm T - S_B) + P_R - Q - E = e \pm \Delta S$$

and the daily balance by

$$(2) \qquad M + P_R - E - Q = e \pm \Delta S$$

where P is precipitation and subscripts S and R refer to snowfall and rainfall respectively, T is blowing snow transport into or out of the basin, S_B is sublimation during blowing snow, M is melt distributed over the snowcovered areas, Q is stream discharge, E is evaporation from snow

free areas, ΔS is change in storage, and e is an error term. Components have units of mm. All components on the left hand side of each equation were measured or calculated, while the terms on the right side are calculated as the residual.

Snow accumulation and melt

Siksik Creek accumulates snow from a larger area than its "drainage basin". Because of relatively irregular terrain, it is a net sink of blowing snow within the Trail Valley Creek area and hence, despite sublimation losses, accumulates more snow than there is direct snowfall on the basin. This is demonstrated in Figure 3, where snowfall on the basin is 190 mm and modelled accumulation is 207 mm SWE. When one considers the loss of snow due to sublimation (average of 34 mm SWE over the basin) then the net basin transport (51 mm SWE) represents a substantial snow water import to the basin. In terms of basin area without this transport import, the "snow contributing area" is one-third larger than the actual basin area. Clearly using only snowfall and basin area to define the basin snow water equivalent before melt is an inadequate technique in the Arctic. The basin wide fluxes as a percentage of final basin snow accumulation are shown in Table 3. Over the basin, sublimation loss represents one-sixth, net transport represents one-quarter and corrected snowfall over 90% of final accumulation. These figures are not representative of local terrain where on level areas sublimation fluxes are much higher.

Table 3 -Calculated fluxes for each terrain type.

	Sublimation (%)	Transport (%)	Precip.	Balance
Tundra	-16	-8	54	29
Highbush	0	5	22	27
Drift	0	28	16	44
Sum	-16	25	92	100

Table 4 illustrates that the snow fall represents 58.1% of the total water inputs to the basin, while blowing snow transport represents 15.6%. Likewise, sublimation during blowing snow events removes 10.4% of basin inputs.

Calculated melt input to the basin is 215 mm (Figure 10), only slightly more that the 207 mm of snow storage.

Table 4 - Annual water balance data for Siksik Ck. (October 1, 1992 to September 30, 1993), expressed in mm and as a % of total water inputs ($P_S + T + P_R = 327$ mm) to the basin. Note that basin snow storage at the end of winter ($P_S + T - S_B$) is equal to 207 mm, larger than snowfall.

Basin	P_S	T	S_B	P_R	Q	E	$e \pm \Delta S$
Siksik Cr.	190	51	34	86	98	203	-8
Inputs	58.1%	15.6%	------	26.3%	------	--------	
Outputs	-----	--------	10.4%	--------	30.0%	62.1%	-2.5%

Runoff

The processes responsible for variable snow depths, percolation into cold snow, frozen soil infiltration, and low initial melt rates, result in a delay of 10 days between the beginning of melt on May 15 (JD 135) and the initiation of Siksik Creek streamflow on May 24 (Day 144) (Figure 5). A total of nearly 150 mm of melt was required to initiate runoff. After this time, discharge increased rapidly, rising to a peak on June 2 (Day 153), after which discharge gradually decreased (Figure 5). Diurnal discharge patterns ceased by June 18 (Day 169). During this period, snowmelt varied greatly, with peak melt rates occurring over the period May 25 to 29 (JD 145 - 149). During this period, basin snowcover was decreasing rapidly, with a snowcovered area of 67% when discharge began (JD 144), 11% by the time of peak discharge (JD 153), and only 5% by the time diurnal fluctuations in response to snowmelt were not obvious in the Siksik record (JD 169). It is interesting to note that the peak snowmelt

contribution to the basin occurred on May 26 (JD 146), with a melt rate of 60 mm/day and a snowcovered area of 48%. This was prior to the peak Siksik Creek discharge.

For Siksik Creek, 37 mm of runoff, or 37.5% of the annual runoff, occurred by the time of the peak discharge, and 92 mm (93.5%) by the time that diurnal fluctuations ceased. For the remainder of the summer the discharge was very small, with only small responses to rain events. Although most of annual runoff occurs during the melt period, discharge only removed 44 % of the snow stored in the basin at the end of winter. The remainder of the snowmelt water entered storage during the melt period (Figure 10), and was used to supply water to evaporation for the remainder of the summer. Since runoff is fairly small, it accounts for only 30% of the total water inputs to the basin on an annual basis.

Figure 10. Calculated daily water balance for Siksik Basin.

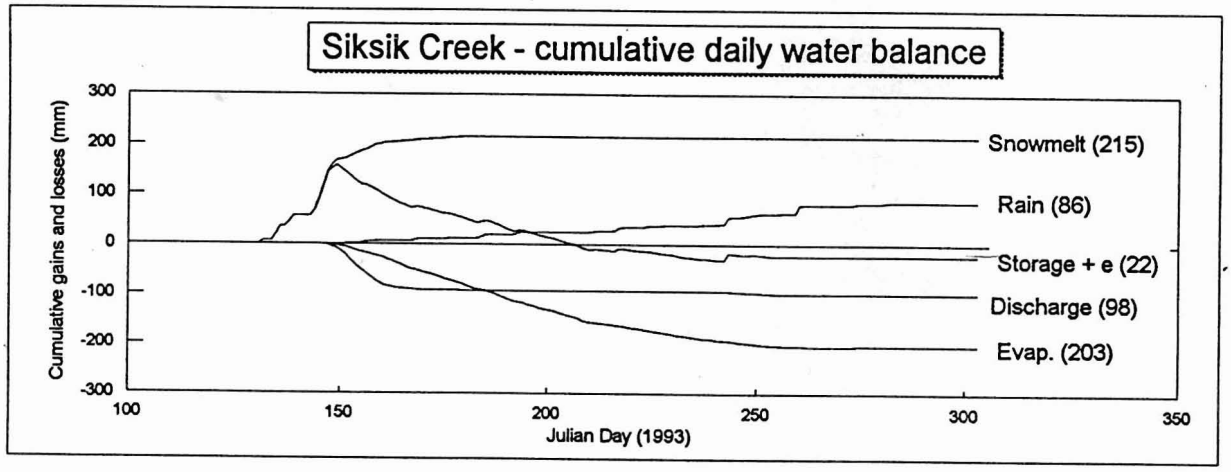

Evaporation

Comparison of lysimeter evaporation to Priestley-Taylor equilibrium evaporation (α=1), showed large spatial and temporal variations in α. Average α varied from 0.16 for a lichen crested hummock, to 0.82 for a hummock with herbs, berries, and graminoids. Although, higher values may be expected due to wetter ground cover following melt, the large ground heat fluxes limited the available energy. As a result, there was only a slight change in α over the summer, with slightly higher values following snowmelt. Over the summer period, the average value of α

was 0.6 for the various land types samples. This value was used in the evaporation calculations.

On an annual basis, evaporation was 213 mm, but when adjusted to account for the snow covered area during the melt period, this was reduced to 203 mm or approximately 1.2 mm/day for the entire summer. Evaporation therefore accounts for 62% of the total water inputs to the basin (Table 4). On a daily basis, it is clear that evaporation begins around day 150 with the first bare ground, but that its magnitude is limited by the small snowfree area. Evaporation then gradually increases, reaching a maximum in mid-summer, after which time it gradually declines (Figure 10).

Storage

The annual water balance suggests that for the 1992/93 water year, Siksik basin had only a small change in water storage. In fact, given the errors involved in the measurements and calculations, it appears that the basin did not undergo any significant changes in storage during the year. Given the nature of the basin with: (a) a shallow active layer, (b) hummocky terrain with mineral areas that would experience slow changes in storage due to low hydraulic conductivity, and highly permeable organic water tracks which drain easily between input events, and (c) no lakes, this basin has little storage capacity.

On a daily basis, however, the basin undergoes large changes in storage (Figure 10). During the melt period, significant melt occurs before the initiation of streamflow, primarily due to the processes of wetting front advance severely delays runoff during the early phases of melt, and soil infiltration. These processes account for a 13 day delay between the start of melt and the start of runoff. During this period, the storage of water increases dramatically, with an estimated storage of nearly 150 mm of water by JD 150. Streamflow and evaporation are small during this period, but rapidly decrease basin storage after JD 150. Storage continues to decrease over the rest of the summer. Figure 10 illustrates that on a daily basis the storage plus error term are negative for much of the summer period with a final value of -22 mm by the end of summer.

(8) CONCLUSION

1. Given simple meterological inputs, the Arctic Blowing Snow Model accurately predicted the

snowcover on each terrain class at the end of winter, and the basin snow storage at the end of winter.

2. Estimated blowing snow transport was a major factor limiting snow on tundra areas, while increasing snowcover at high bush and drift sites. In addition, sublimation was a major factor in removing snow from the tundra areas.

3. A snow percolation model demonstrated the delay between the start of melt, and the availability of meltwater at the base of the snowpack. In addition, it was able to estimate the time for each terrain type when the snowpack was not contributing, partially contributing, and full contributing water to runoff.

4. Mineral earth hummocks promote preferential flow through the interhummock zone, with subsurface flow velocities governed by the size, density and distribution of hummocks, and whether conducting macropores are present.

5. By maintaining hillslope water table levels close to the surface, where hydraulic conductivity is high, a late lying snow drift enables rapid subsurface flow velocities

6. Using modelled and estimated parameters illustrated the magnitudes of the annual water balance. This showed that for a small basin, blowing snow transport was a significant input of water to the basin (15%), while snowfall accounted for 58% of annual input. Of these inputs, 10% sublimated during blowing snow, 62% evaporated, and only 30% was available for runoff.

7. Daily water balance estimates showed that approximately 150 mm of melt was required before streamflow began, and that snowmelt runoff accounted for only 44% of snowcover. The rest filled water storages, and was evaporated during the remainder of the summer.

Acknowledgments

We would like to thank Cuyler Onclin and Joni Onclin for the help in collecting and analyzing the field data, and Natasha Neuman for developing the landscape maps of TVC. Kevin Shook kindly allowed us to use his air photos taken during the 1993 melt period for determining snow covered area. The Inuvik Scientific Research Centre, Science Institute of the NWT and Polar Continental Shelf Project for their essential field and logistical support. This project was partially funded by the Environment Canada's Green Plan support of the Canadian GEWEX Programme.

References

Aagaard, K. and E.C. Carmack. 1989. The role of sea ice and other fresh water in the Arctic circulation. Jour. Geophys. Res., 94, 14,485 - 14,998.

Atmospheric Environment Service. 1982a. Canadian Climate Normals - Volume 2 Temperature, 1951-1980. Environment Canada, 306 pp.

Atmospheric Environment Service. 1982a. Canadian Climate Normals - Volume 3 Precipitation, 1951-1980. Environment Canada, 602 pp.

Benson, C.S. 1982. Reassessment of winter precipitation on Alaska's Arctic slope and measurements on the flux of wind blown snow. Report No. 288, Geophysical Institute, University of Alaska, Fairbanks, 26 pp.

Brown, T. and J.W. Pomeroy. 1989. A blowing snow detection gauge. Cold Region Science and Technology. 16, 167-174.

Chason, D. B. and D.I. Siegel, 1986. Hydraulic conductivity and related physical properties of peat, Lost River Peatland, Northern Minnesota. Soil Science, Vol. 142, No. 2.

Church, M.J. 1974. Hydrology and permafrost with reference to northern North America. In - Permafrost Hydrology, Proceedings of Workshop Seminar 1974, Canadian National Committee for the International Hydrological Decade, Ottawa, Ontario, 7-20.

Dunne, T., A.G. Price, and S.C. Colbeck. 1976. The generation of runoff from subarctic snowpacks. Water Resources Research, 12, 677-685.

Farrell, R,E., G.D.W. Swerhone, and C. van Kessel, 1991. Construction and evaluation of a reference electrode assembly for use in monitoring in situ soil redox potentials. Commun. In Soil Sci. Plant Anal., 22 (11&12), 1059-1068.

Goodison, B.E. 1978. Accuracy of Canadian snow gauge measurements. J. Applied Meteorology, 27, 1542-1548.

Heginbottom, J.A. and L.K. Radburn (comp.). 1992. Permafrost and ground ice conditions of northwestern Canada. Geological Survey of Canada, Map 1691A, scale 1:1 000 000.

Heron, R. and Woo, M-K. 1978. Snowmelt computations for a high Arctic site. Proceedings 35th Eastern Snow Conference, 162-172.

IPCC. 1990. Climate Change, The IPCC Scientific Assessment. J.T. Houghton, G.J. Jenkins, and J.J. Ephraums (Eds.). Cambridge Univ. Press, Cambridge, U.K., 365 pp.

Mackay, J.R. 1980. The origin of hummocks, western Arctic Coast, Canada. Can. Jour. Earth Science, 17, 996-1006.

Marsh, P. and J.W. Pomeroy. 1994. Snow/soil heat and mass fluxes at an Arctic treeline site. European Conference on the Global Energy and Water Cycle. July 1994, Royal Society, London.

Marsh, P. 1991. Water flux in melting snow covers. In - Advances in Porous Media, Vol. 1. M.Y. Corapcioglu (ed.). Elsevier, Amsterdam, 61-124.

Marsh, P. and W.L. Quinton, 1993. Snowmelt Infiltration and Sub-surface flowpaths in frozen soils: field evidence from a continuous permafrost site. In: Proceedings of Canadian Geophysical Union, annual meeting of the Hydrology Section, Banff, Canada.

Marsh, P. and M.-K. Woo. 1981. Snowmelt, glacier melt, and high arctic streamflow regimes. Canadian Journal of Earth Sciences, 18, 1380-1384.

Marsh, P. and M-K. Woo. 1984a. Wetting front advance and freezing of meltwater within a snowcover 1: Observations in the Canadian Arctic. Water Resources Research, 20, 1853-1864.

Marsh, P. and M-K. Woo. 1984b. Wetting front advance and freezing of meltwater within a snowcover 2: A simulation model. Water Resources Research, 20, 1865-1874.

Marsh, P. and M-K. Woo. 1993. Infiltration of meltwater into frozen soils in a continuous permafrost environment. Proc. International Permafrost Conference, China, 443-338.

Moore, R.D. 1983. On the use of bulk aerodynamic formulae over melting snow. Nordic Hydrology, 14, 193-206.

Pomeroy, J.W., P. Marsh, and L. Lesack. 1993a. Relocation of major ions in snow along the tundra-taiga ecotone. *Nordic Hydrology*, 24, 151-168.

Pomeroy, J.W., D.M. Gray, and P.G. Landine. 1993b. The Prairie Blowing Snow Model: Characteristics, validation, operation. Journal of Hydrology, 144, 165-192.

Pomeroy, J.W. and D.M. Gray. 1994. Sensitivity of snow relocation and sublimation to climate and surface vegetation. In - Proceedings of Yokohama Symposium. Snow-Climat-Vegetation, IAHS Press, Wallingford. Jones, H.G. and T. Davies (ed.), in press.

Pomeroy, J.W., P. Marsh, and D.M. Gray. 1994. Snow accumulation and sublimation at the tundra-taiga transition. European Conference on the Global Energy and Water Cycle. July 1994, Royal Society, London.

Priestley, C.H.B. and Taylor, R.J. 1972. On the assessment of surface heat flux and evaporation using large-scale parameters. Monthly Weather Review, 100, 81-92.

Quinton, W.L. 1991. The hydrology of a subarctic patterned wetland. York University, M.Sc., 141pp.

Rampton, V.N. 1974. Surfical Geology Aklavik. Geological Survey of Canada. Map 31-1979, 1:250,000.

Roulet, N.T. and M-K. Woo. 1986. Hydrology of a wetland in the continuous permafrost region. Jour. of Hydrology, 89, 73-91.

Rouse, W.R., S.G. Hardill, and P. Lafleur. 1987. The energy balance in the coastal environment of James Bay and Hudson Bay during the growing season. Journal of Climatology, 7, 165-179.

Rouse, W.R. 1984. Microclimate of arctic tree lines, 2. Soil microclimate of tundra and forest. Water Resources Research, 20, 67-73.

Shook, K., D.M. Gray, and J.W. Pomeroy. 1993. Geometry of patchy snow covers. Proceedings 50th Eastern Snow Conference, Quebec, 89-96.

Steppuhn, H. and G.E. Dyck. 1974. Estimating true basin snowcover. In - Advanced Concepts and Techniques in the study of snow and ice resources. National Academy of Sciences, U.S. International Hydrological Decade, Washington, D.C., 314-324.

Woo, M.-K., R. Heron, P. Marsh, and P. Steer. 1983. Comparison of weather station snowfall with winter snow accumulation in High Arctic basins. *Atmosphere-Ocean*, 21, 312-325.

Woo, M. -K. 1990. Permafrost hydrology. in: T.D. Prowse and C.S.L. Ommanney (ed.), Northern Hydrology: Canadian Perspectives. NHRI Science Report No. 1, Environment Canada, National Hydrology Research Institute, 63-76.

Wright, R.K. 1981. The water balance of a lichen tundra underlain by permafrost. McGill Subarctic Research Paper No. 33, Climatological Research Series No. 11, Centre for Northern Studies, McGill University, Montreal, Quebec, 110 pp.